



Crystal structure, chemical bond and enhanced performance of β -Zn₄Sb₃ compounds with interstitial indium dopant



Dingguo Tang^{a,b}, Wenyu Zhao^{a,*}, Jian Yu^a, Ping Wei^a, Hongyu Zhou^a, Wanting Zhu^a, Qingjie Zhang^{a,*}

^a State Key Laboratory of Advanced Technology for Materials Synthesis and Processing, Wuhan University of Technology, Wuhan 430070, China

^b Key Laboratory of Catalysis and Materials Science of the State Ethnic Affairs Commission & Ministry of Education, South-Central University for Nationalities, Wuhan 430074, China

ARTICLE INFO

Article history:

Received 8 December 2013

Received in revised form 8 February 2014

Accepted 11 February 2014

Available online 18 February 2014

Keywords:

Zinc antimonide

Indium doping

Crystal structure

Chemical bond

Thermoelectric performance

ABSTRACT

In-doped β -Zn₄Sb₃ compounds (Zn_{4-x}In_xSb₃, 0 ≤ x ≤ 0.24) were prepared by melt-quenching and spark plasma sintering technology in the work. The resultant samples were systematically investigated by X-ray diffraction, X-ray photoelectron spectroscopy, differential scanning calorimetry and thermoelectric property measurements. The In dopant was identified to preferentially occupy the interstitial site in β -Zn₄Sb₃ and led to the local structural perturbations near the 12c Sb2 and 36f Zn1 sites. The Auger parameters of Zn and Sb indicated that the increase in the valence of Zn was attributed to the charge transfer from Zn to In atoms. The binding energies of In 3d_{5/2} core level showed that the interstitial In dopant was *n*-type dopant (In³⁺) in slightly In-doped Zn_{4-x}In_xSb₃, but acted as acceptor and was *p*-type dopant (In⁺) in heavily In-doped ones. The discovery provides a reasonable explanation for the puzzled relation between σ and x for Zn_{4-x}In_xSb₃. Simultaneously increasing the electrical conductivity and Seebeck coefficient of Zn_{4-x}In_xSb₃ can be realized through the local structural perturbations. The significantly enhanced power factor and the intrinsic low thermal conductivity resulted in a remarkable increase in the dimensionless figure of merit (*ZT*). The highest *ZT* reached 1.41 at 700 K for Zn_{3.82}In_{0.18}Sb₃ and increased by 68% compared with that of the undoped β -Zn₄Sb₃.

© 2014 Published by Elsevier B.V.

1. Introduction

Thermoelectric (TE) materials have been in global interest for the sake of energy efficiency and environmental impacts for the past decades [1,2]. The efficiency of TE conversion depends on the dimensionless figure of merit, $ZT = \alpha^2 \sigma T / \kappa$, where α is the Seebeck coefficient, σ the electrical conductivity, T the absolute temperature, and κ the total thermal conductivity ($\kappa = \kappa_C + \kappa_L$, where κ_C is the carrier contribution and κ_L the lattice contribution). The *ZT* of β -Zn₄Sb₃ is as large as 1.3 at 670 K, which makes it can be used in high-efficient TE generators for waste heat recovery and automobile industry applications in the intermediate temperature range (500–700 K) [3,4]. Moreover, cheap, non-toxic and abundant resources of zinc and antimony are in favor of large-scale commercial applications of β -Zn₄Sb₃ [5,6]. The high *ZT* of β -Zn₄Sb₃ originates from the exceptional low κ_L , e.g. 0.65 W m⁻¹ K⁻¹ at 300 K, which is much lower than those of the state-of-art *p*-type TE materials [3]. The low κ_L is essentially attributed to the strong

phonon scattering due to the complicated crystal structure. The core structure of β -Zn₄Sb₃ contains three distinct atom sites 36f Zn1, 18e Sb1, and 12c Sb2 in space group *R*3̄c, and the 18e Sb1 site may be occupied by Zn and Sb atoms simultaneously [7,8]. Snyder et al. proposed the three-interstitial model, suggesting that there is no evidence of Zn substitution for Sb at the 18e Sb1 site [9]. The Zn atoms may randomly occur at the interstitial sites besides the 36f Zn1 site, which was also established by Rauwel et al. with the presence of nanovoids in the β -Zn₄Sb₃ system due to solid-state diffusion of Zn [10]. The disordered structure gave a reasonable explanation for the low κ_L of β -Zn₄Sb₃.

Many attempts to decrease the κ of β -Zn₄Sb₃ by increasing the structure disorders with dopant have been reported. Nylén et al. and Litvinchuk et al. indicated that the trace metal dopant at the Zn site could remarkably decrease the κ_L [11,12]. The In and Cd doping were reported to decrease the κ of (Zn_{0.995}In_{0.005})₄Sb₃ and (Zn_{0.99}Cd_{0.01})₄Sb₃ [13,14]. Qin and Pan et al. reported that some doping elements (Bi, Ag) at the Zn sites might remarkably reduce the κ of β -Zn₄Sb₃ [15,16]. Besides at the Zn site, elemental doping at the Sb site was also implemented to decrease the κ of β -Zn₄Sb₃. Zhou et al. indicated that Bi dopant could decrease effectively the κ_L of Zn₄Sb_{3-x}Bi_x [17]. Li et al. found that the Te substitution for Sb reduced the κ under the temperature from 300 to 650 K [18].

* Corresponding authors. Address: No. 122, Luoshi Road, Wuhan 430070, China. Tel./fax: +86 27 87651843.

E-mail addresses: wyzhao@whut.edu.cn (W. Zhao), zhangqj@whut.edu.cn (Q. Zhang).

We recently discovered that the preferential substitution of In dopant for one Sb atom of Sb_2 dimer resulted in the remarkable decrease in the κ_L of $\beta\text{-Zn}_4\text{Sb}_3$ [19]. These researches reveal that the κ of $\beta\text{-Zn}_4\text{Sb}_3$ can be further decreased by doping. However, with the lower limit of theoretical value of glass-state for the κ_L , the reduction in the κ is not satisfied for $\beta\text{-Zn}_4\text{Sb}_3$ to significantly improve TE performance.

On the other hand, ZT benefits from excellent electrical transport properties. High σ and/or big α can be achieved through carrier concentration optimization and band structure engineering [20,21]. Elemental doping is regarded as a powerful way to optimize electrical transport properties. Some exciting work has been reported to increase α by properly element doping in TE compounds, e.g. Tl-doped PbTe [22] and Sn-doped Bi_2Te_3 [23]. Wang et al. indicated that the Ge doping resulted in a great increase in the α for Ge-doped Zn_4Sb_3 [24]. In the paper, we reported that the remarkable increases in α and σ could be simultaneously realized by doping the In dopant at the interstitial site in $\beta\text{-Zn}_4\text{Sb}_3$. The largest ZT value of 1.41 at 700 K was obtained due to the significantly enhanced power factor ($\alpha^2\sigma$) and the intrinsic low κ for $\text{Zn}_{3.82}\text{In}_{0.18}\text{Sb}_3$ compound. It shows that the great improvement in thermoelectric performances for $\beta\text{-Zn}_4\text{Sb}_3$ can be achieved by a small amount of In doping although the In metal is scarce. Our results showed that the In dopant preferentially occurred at the interstitial Zn site and led to the local structural perturbations near the 12c Sb2 and 36f Zn1 sites. The interstitial In dopant was n -type dopant (In^{3+}) in slightly In-doped $\text{Zn}_{4-x}\text{In}_x\text{Sb}_3$, but acted as acceptor and was p -type dopant (In^+) in heavily In-doped ones. The crystal structure and bonding characteristics of the In-doped $\text{Zn}_{4-x}\text{In}_x\text{Sb}_3$ have been carefully investigated to reveal the effects of the In dopant on the TE properties.

2. Experimental

2.1. Sample preparation

The highly pure metals of Zn (99.999%, powder), Sb (99.99%, powder) and In (99.99%, powder) were used as raw materials. The mixtures of raw materials with nominal compositions $\text{Zn}_{4-x}\text{In}_x\text{Sb}_3$ ($0 \leq x \leq 0.24$) were sealed into a silica tube under vacuum. The tube was heated up to 1023 K and then kept for 2 h, then quenched in cool oil. The obtained ingots were ground into fine powders and sintered into polycrystalline bulk materials by spark plasma sintering (SPS) at 673 K for 3 min in an alloy die.

2.2. XRD measurement

The bulk materials were ground into uniform powders for X-ray diffraction (XRD). XRD data were recorded by Bruker D8 Advance diffractometer with $\text{Cu K}\alpha$ radiation. The accelerating voltage, applied current, scanning speed, step-by-step scanning size, DS-SS-RS slit, and scanning range were 40 kV, 40 mA, 4.2 deg/min, 0.02° , 1.0° – 1.0° – 0.3 mm, and 10 – 135° , respectively. Rietveld refinements of the XRD data based on the three-interstitial model [9] were carried out using GSAS [25] and EXPGUI [26] softwares.

2.3. XPS measurement

The bulk materials were cut into circular sheets of $8\text{ mm} \times 2\text{ mm}$ (diameter \times thickness) for X-ray photoelectron spectroscopy (XPS) analysis. The sheets were polished carefully to ensure flat and smooth surface, and washed in acetone by an ultrasonic cleaner. They were dried in N_2 stream and then transferred into the apparatus. XPS spectra were recorded by Thermo VG Multilab 2000 spectrometer under a vacuum of 3×10^{-7} Pa. The radiation source is $\text{Mg K}\alpha$ ($h\nu = 1253.6\text{ eV}$) with a power of 400 watts. Survey scans were performed at pass energy of 100 eV and step size of 1 eV, while the pass energy of 25 eV and step size of 0.05 eV were adopted for the narrow scans of Zn $2p_{3/2}$, Sb $3d_{5/2}$, In $3d_{5/2}$, Zn L_{3MM} and Sb M_{4NN} . The C 1s photoelectron peak of the adventitious carbon at 284.6 eV was used as a reference for charge shift calibration. The In 3d spectra were first treated by employing the *Avantage* software to subtract the background with a Shirley type and then smoothed by Savitzky–Golay method. The Auger parameter of Zn (or Sb) was calculated by adding the binding energy of photoelectrons for Zn $2p_{3/2}$ (or Sb $3d_{5/2}$) and the kinetic energy of Auger electrons for Zn L_{3MM} (or Sb M_{4NN}).

2.4. Thermoelectric property measurement

The bulk materials were cut into square or circular sheets and strips for thermoelectric property measurements. The sheets and strips from the same SPS bulk material were used to evaluate the performances of a certain sample. Only pure phase samples were chosen for thermoelectric property measurements, avoiding the influences from the secondary phase. The σ and α were simultaneously measured using commercial equipment (ZEM-3, Sinkuriko) under a low pressure inert gas (He) atmosphere. The κ was calculated using the equation $\kappa = \lambda\rho C_p$, where λ is the thermal diffusivity coefficient, ρ the density of bulk material and C_p the specific heat capacity. The λ was measured by a laser flash technique (Netzsch LFA 427) in a flowing Ar atmosphere. The ρ was obtained by the Archimedes method. The C_p was measured using differential scanning calorimeter (DSC, TA Q20). The detail data of ρ and C_p were list in Table SI as supporting information. The κ_L was obtained by subtracting the carrier contribution from κ using the equation $\kappa_L = \kappa - \kappa_C$. Here, the κ_C is expressed by the Wiedemann–Franz equation $\kappa_C = \sigma LT$, where L is the Lorenz number with a value of $2.0 \times 10^{-8}\text{ V}^2\text{K}^{-2}$ for degenerate semiconductor [27]. The low-temperature DSC curves in the temperature range of $200 \sim 300\text{ K}$ were measured under a heating rate of 5 K min^{-1} .

3. Results and discussion

3.1. Crystal structure

Fig. 1 shows XRD patterns of the In-doped $\text{Zn}_{4-x}\text{In}_x\text{Sb}_3$ ($0 \leq x \leq 0.24$). It can be seen that the diffraction peaks of all the samples can be identified as rhombohedral structure of $\beta\text{-Zn}_4\text{Sb}_3$ with space group $R\bar{3}c$. The secondary phase of Zn can be found when $x = 0.21$ and 0.24. The lattice parameters of the In-doped samples are shown in Fig. 2. The a and c values increase monotonically with the x in the range of 0–0.18, and keep constant when $x > 0.18$. It means that the crystal lattice of $\text{Zn}_{4-x}\text{In}_x\text{Sb}_3$ does not expand when the doping content of In dopant is higher than $x = 0.18$, which indicates that the solubility limit of In dopant in $\text{Zn}_{4-x}\text{In}_x\text{Sb}_3$ is about $x = 0.18$. An In rich secondary phase of InSb [13] should exist along with Zn secondary phase when $x > 0.18$. However, InSb is not obvious in the XRD patterns of Fig. 1, which may be due to its low concentration below the XRD detection limit. A significant shift of the peak near $2\theta = 25.2^\circ$ toward lower angle is found with increasing the x in the range of 0–0.18, as shown in the inset of Fig. 1, which reveals the increment of interplanar spacing of (300) face. The 2θ shift confirms that the In dopant has entered into the lattice of $\beta\text{-Zn}_4\text{Sb}_3$.

To determinate the crystallography site of the In dopant in the In-doped $\text{Zn}_{4-x}\text{In}_x\text{Sb}_3$, low-temperature thermal analysis was carried out. The typical DSC curves of $\text{Zn}_{4-x}\text{In}_x\text{Sb}_3$ during the cooling (a, b, c) and heating (a', b', c') processes are shown in Fig. 3. A pair of endo- and exo-thermic peaks near 260 K is observed for $\beta\text{-Zn}_4\text{Sb}_3$, but similar phenomenon has not been observed for the In-doped samples. It is well known that the thermal effect is

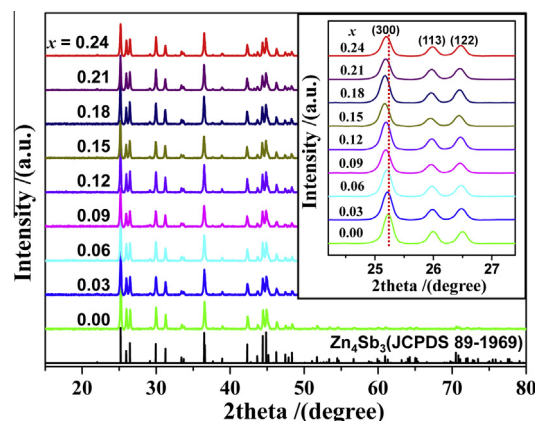


Fig. 1. XRD patterns of In-doped $\text{Zn}_{4-x}\text{In}_x\text{Sb}_3$.

Download English Version:

<https://daneshyari.com/en/article/1611233>

Download Persian Version:

<https://daneshyari.com/article/1611233>

[Daneshyari.com](https://daneshyari.com)